

Original Article

Masquelet's induced membrane promotes the osteogenic differentiation of bone marrow mesenchymal stem cells by activating the Smad and MAPK pathways

Qian Tang^{1*}, Minji Tong^{1*}, Gang Zheng¹, Liyan Shen¹, Ping Shang², Haixiao Liu¹

Departments of ¹Orthopaedic Surgery, ²Rehabilitation, The Second Affiliated Hospital and Yuying Children's Hospital of Wenzhou Medical University, 109, Xueyuanxi Road, Wenzhou 325027, China. *Equal contributors.

Received November 3, 2017; Accepted February 12, 2018; Epub April 15, 2018; Published April 30, 2018

Abstract: The Masquelet's induced membrane (IM) technique is widely used to treat large segmental bone defects due to its physical priority and biological function. However, the underlying molecular mechanism of the IM on bone formation remains unknown. In the present study, rat bone marrow-derived mesenchymal stem cells (BMSCs) were used as an *in vitro* model and bone morphogenetic protein 2 (BMP-2) was used as a positive control to evaluate the effects of the IM on the osteogenic differentiation of BMSCs. Although the IM group did not exhibit a significant increase in the expression of Runt-related transcription factor 2 (Runx2), Collagen I (Col I), osteocalcin (OCN) and alkaline phosphatase (ALP) relative to the BMP-2 administration, the IM was considerably effective compared with the untreated group. Mechanistically, we found that the IM activated the Smad and mitogen-activated protein kinase (MAPK) pathways, which was further confirmed by application of specific inhibitors of Smad1/5/8 (LDN-193189) and ERK1/2 (U0126). After the combined treatment of the IM and LDN-193189 as well as U0126, the IM-induced increase in Runx2, Col I, and OCN expression was significantly inhibited. These results suggest that IM promotes the osteogenic differentiation of rat BMSCs by activating the Smad1/5/8 and MAPK pathways.

Keywords: Masquelet, induced membrane, Smad, MAPK, osteogenesis

Introduction

The induced membrane (IM) technique was first described by Masquelet et al. in 1986 who developed the concept of IM development and reconstructed large defects by combined application of this functional induced membrane with non-vascularized bone autografts [1, 2]. The IM technique is a valid alternative strategy used for the reconstruction of long bone defects, especially those resulting from major trauma, surgical excision of tumors and debridement after post-traumatic septic non-unions or osteitis [3-5]. This technique consists of two stages of surgery: firstly, a polymethylmethacrylate (PMMA) cement spacer is implanted inside the defect area to trigger a reactive IM with bone healing properties. Secondly, after implantation for 6-8 weeks, the spacers are removed, followed by autologous bone filling [6, 7]. By applying this technique in clinical prac-

tice, large bone defects occurring in the humerus, ulna, wrist, hand, femur, tibia, and even in the mandible, can achieve satisfactory healing [8-12].

Historically, the IM consists of a fibrous inner layer (closest to the PMMA spacer) and an outermost vascularized layer (furthest from the spacer) [13]. This membrane not only acts as a capsule to contain bone graft and to prevent fibrous tissue ingrowth into the defect site but also exerts important biological properties to favor bone formation [14]. Several functional proteins secreted from this functional membrane during membrane formation, such as bone morphogenetic protein 2 (BMP-2), transforming growth factor- β (TGF- β), vascular endothelial growth factor A (VEGF-A), and von Willebrand factor (vWF), are involved in osteoblast proliferation and differentiation [13-15]. However, the precise mechanism by which the IM mediates osteogenesis remains unclear.

Bone marrow-derived mesenchymal stem cells (BMSCs) are multipotent cells with self-renewal ability and exhibit directional differentiation under appropriate stimulation [16]. Since BMSCs are easily extracted and exhibit differentiation potential, cultured BMSCs are widely used *in vitro* to evaluate factors that contribute to osteogenesis [17]. Moreover, the canonical Smad pathway and mitogen-activated protein kinase (MAPK) cascades are two well-studied signaling pathways that regulate BMSCs differentiation during skeletal development [18-20]. Both signaling cascades converge at certain transcription factors (e.g., Runx2) to promote osteoblast differentiation from mesenchymal precursor cells [20]. Besides, it is important to note that TGF- β and BMP-2 are two major promoters involved in the induction of the Smad and MAPK pathways and the IM is a natural carrier of BMP-2 and TGF- β [15, 20]. Therefore, we hypothesized that the underlying mechanism by which the IM acts on bone formation is associated with activation of the Smad and MAPK pathways. In this study, we examined, for the first time, the effects of the IM on the osteogenic differentiation of BMSCs and investigated the mechanism involved.

Materials and methods

Reagents and antibodies

Recombinant rat BMP-2 protein was purchased from Peprotech (NJ, USA); LDN-193189 and U0126-EtOH were purchased from Aladdin (Shanghai, China). The primary antibodies against BMP-2, TGF- β , collagen I, and β -actin were acquired from Abcam (Cambridge, UK); anti-Smad1/5/8 and -osteocalcin (OCN) antibodies were obtained from Santa Cruz Biotechnology (CA, USA); anti-Runx2 antibody, goat anti-rabbit, and anti-mouse IgG-horseradish peroxidase (HRP) antibodies were obtained from Bioworld (OH, USA); and antibodies against p-ERK1/2, ERK1/2, p-p38, p38, p-JNK, JNK, and p-Smad1/5/8(9) were purchased from Cell Signaling Technology (MA, USA). All cell culture reagents were purchased from Gibco (NY, USA).

Animal model

Ten Sprague-Dawley rats of mean weight 350 g were purchased from the Animal Center of the Chinese Academy of Sciences, Shanghai,

China. All animal care and use procedures adhered to the Guide for the Care and Use of Laboratory Animals of the National Institutes of Health and the study was approved by the Animal Care and Use Committee of Wenzhou Medical University (ethics code: wydw2014-0129). Critical segmental defects were created in the right femur using the model reported by Henrich et al. [13]. After intraperitoneal injection of 2% (w/v) pentobarbital (40 mg/kg), all rats were placed in the left lateral prone position, and a 40-mm longitudinal incision was made over the lateral aspect of the right thigh. Then, the biceps femoris and vastus lateralis muscles were separated to expose the lateral aspect of the al bone. A six-hole, 1.0-mm-thick titanium mini-plate (F215002.T01, Fengyi, Tianjin, China) was applied to the lateral aspect of the femoral shaft and secured in place using four 1.5-mm-long cortical screws. A critical-sized defect 10 mm in length was induced using a reciprocating saw, followed by filling with a 10-mm-diameter PMMA cement cylinder molded *ex vivo*. The wound was irrigated with sterile saline, the muscles and the fascia were carefully re-approximated using 4-0 Vicryl sutures, and the skin was closed with 3-0 silk sutures. Six weeks later, X-rays were taken to determine the position of the PMMA spacer. If no significant spacer shift was evident, the IM that had formed around the spacer was collected for further experiments.

Histology

The induced membrane samples were collected 6 weeks after surgery. After dehydration and embedding in paraffin, the tissues were cut into 5- μ m-thick sagittal sections and the slides stained with hematoxylin and eosin (H&E). For immunohistochemical staining, the sections were further incubated with 0.4% (w/v) pepsin (Sangon Biotech, Shanghai, P. R. China) in 5 mM HCl at 37°C for 20 min (antigen retrieval) and nonspecific binding was blocked by incubation in 10% (w/v) bovine serum albumin for 30 min at room temperature. Sections were then incubated with primary antibodies (anti-BMP-2, 1:100 and anti-TGF- β , 1:100) overnight at 4°C. Finally, the sections were incubated with appropriate HRP-conjugated secondary antibodies (Santa Cruz Biotechnology, TX, USA), and examined and photographed under a microscope (Olympus, Japan).

Induced membrane and osteogenic differentiation

Protein extraction from induced membranes

The induced membranes collected from bone defect site after 6 weeks of surgery were rapidly stored at -80°C for western blotting. Briefly, frozen animal membrane tissues homogenized in ice-cold RIPA lysis buffer (containing 50 mM Tris-HCl pH 8.0, 150 mM NaCl, 1% NP-40, 0.5% deoxycholate, 0.1% SDS, 10 mM $\text{Na}_2\text{P}_2\text{O}_7$, 10 mM NaF, 1 mg/ml aprotinin, 10 mg/ml leupeptin, 1 mM sodium vanadate) and 1 mM PMSF (Phenylmethanesulfonyl fluoride). Tissue homogenates were incubated for 15 min at 4°C and centrifuged at 12,000 rpm, for 15 min at 4°C . The supernatant containing the soluble proteins was recovered. Total proteins in tissue lysates were quantified using the BCA Protein Assay Kit (Beyotime Biotechnology, Shanghai, China) according to the manufacturer's protocol. The quantified protein solutions are used for *in vitro* experiments.

Isolation of primary rat bone marrow mesenchymal stem cells (BMSCs)

Femoral BMSCs were isolated and cultured as described previously [21]. Briefly, after euthanasia, the hind limbs were aseptically removed and the bones dissected free of soft tissue. The marrow cavities of both the femora and tibiae were flushed with Dulbecco's modified Eagle medium (DMEM) medium supplemented with 10% (v/v) fetal bovine serum (FBS) and 1% (w/v) penicillin and streptomycin. The cells were seeded into 25-cm² culture flasks and grown in a humidified atmosphere under 5% (v/v) CO₂ at 37°C . Non-adherent cells were removed by frequent medium changes after 24 h. The remaining adherent cells were cultured for 14 days to 80% confluence and then passaged after digestion with 0.25% (w/v) trypsin for 3 min. Passage 2 cells were used for further experiments.

Cell administration

BMSCs were seeded at 5×10^4 cells/cm² and cultured in completed medium with or without the addition of 100 μg amounts of protein extract from IMs obtained 6 weeks after surgery. After 14 days, the cells were collected and subjected to quantitative reverse transcription polymerase chain reaction (qRT-PCR), western blot analysis, and alizarin red staining. To further explore the effects of Smad1/5/8 and

MAPK pathways on IM-induced osteogenesis, cells were treated with combinations of IM protein and LDN-193189 (100 nM) or U0126 (25 μM).

Real-time polymerase chain reaction

Total RNA of BMSCs treated with IM or BMP-2 was extracted from cells grown in three 6-cm-diameter culture plates, using TRIzol reagent (Invitrogen, CA, USA). Total RNA (1,000 ng) was reverse-transcribed to cDNA (MBI Fermentas, Germany). For quantitative real-time PCR (qPCR), the total reaction volume was 10 μL , including 5 μL of $2 \times$ SYBR Master Mix, 0.25 μL of each primer solution, and 4.5 μL diluted cDNA. The RT-PCR conditions were as follows: 10 min at 95°C , followed by 40 cycles (each 15 s) at 95°C and 1 min at 60°C . Reactions were performed with the aid of a CFX96 Real-Time PCR System (Bio-Rad, CA, USA). The cycle threshold (Ct) values were collected and normalized to the levels of glyceraldehyde 3-phosphate dehydrogenase (GAPDH) level. The related mRNA level of each target gene was calculated using the $2^{-\Delta\Delta\text{Ct}}$ method. Primers amplifying the genes encoding Runx2, collagen I, OCN, and alkaline phosphatase (ALP) were designed with the aid of the NCBI Primer-Blast Tool. (<https://www.ncbi.nlm.nih.gov/tools/primer-blast/>), and were as follows: Runx-2, (F) 5'-TGTCATCTCCAGCCGTGTC-3', (R) 5'-TCTGTCTGTGCCTTCTTGTTTC-3'; Cola1, (F) 5'-GACCTCCGGCTCCTGCTCCT-3', (R) 5'-TCGCACACAGCCGTGCCATT-3'; OCN, (F) 5'-CGGCCCTGAGTCTGACAAA-3', (R) 5'-ACCTTATTGCCCTCCTGCTT-3'; ALP, (F) 5'-AACGTGGCCAAGAATCATCA-3', (R) 5'-TGTCCATCTCCAGCCGTGTC-3'; and GAPDH (F) 5'-AGAAGTGGTGAAGCAGGCGG-3', (R) 5'-ATCCTTGCTGGGCTGGGTGG-3'.

Western blotting

Total BMSC proteins were extracted using radioimmunoprecipitation lysis buffer containing 1 mM phenylmethanysulfonyl fluoride on ice for 10 min followed by 15 min of centrifugation at 12,000 rpm in 4°C ; protein concentrations were measured using a BCA protein assay kit (Beyotime, Jiangsu, China). Proteins (40 ng) were separated via sodium dodecyl sulfate-polyacrylamide gel electrophoresis and transferred to a polyvinylidene fluoride membrane (Bio-Rad). After blocking with 5% (w/v) nonfat milk for 2 h, the membranes were incubated

Induced membrane and osteogenic differentiation

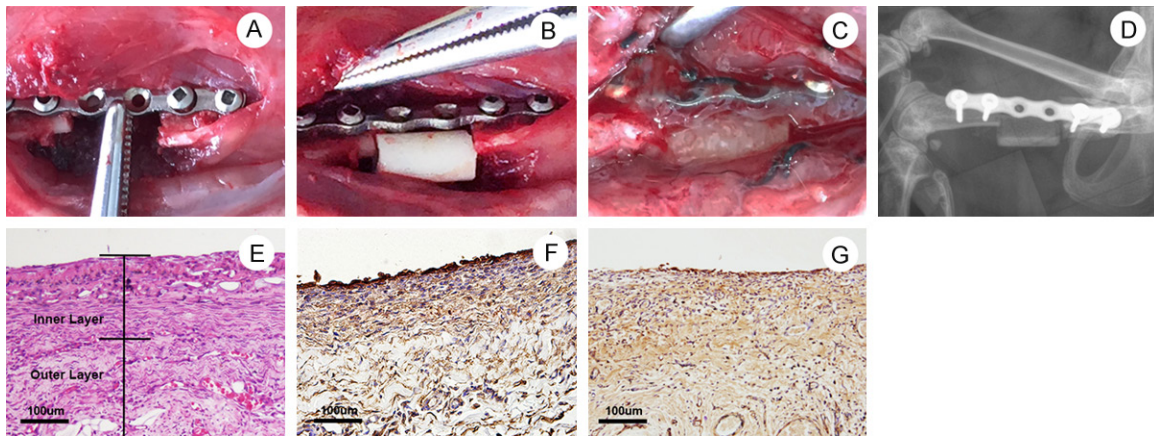


Figure 1. Surgical procedure and characteristics of Masquelet's induced membrane (IM) model in a critical-size femoral defect site. The position of PMMA spacer was determined via digital X-ray machine. The characteristics of IM were assessed via H&E staining and immunohistochemistry. A: A 40-mm incision was made on the right thigh to create a 10-mm defect in femur. B: The polymethylmethacrylate (PMMA) cylinder was inserted into the defect site. C: The IM formed around the PMMA spacer at 6 weeks post-surgery was exposed. D: X-ray image showed correct position of PMMA spacer in the bone defect site at 6 weeks post-surgery. E: H&E staining to observe the inner layer and outer layer of IM formed at 6 weeks post-surgery (Scale bar: 100 μ m). F: Immunohistochemical staining of BMP-2 in the IM at 6 weeks post-surgery (Scale bar: 100 μ m). G: Immunohistochemical staining of TGF- β in the IM at 6 weeks post-surgery (Scale bar: 100 μ m).

with primary antibodies against Runx2 (1:1,000), Collagen I (1:1,000), OCN (1:1,000), p-ERK1/2 (1:1,000), ERK1/2 (1:1,000), p-p38 (1:1,000), p38 (1:1,000), p-JNK (1:1,000), JNK (1:1,000), p-Smad1/5/8 (1:1,000), and Smad1/5/8 (1:250) overnight at 4°C, followed by subsequent incubation with appropriate secondary antibodies for 2 h at room temperature. After three washes with Tris-buffered saline with Tween, the bands were visualized and quantified using Image Lab 3.0 software (Bio-Rad).

Alizarin red staining

We explored osteogenic differentiation of BMSCs. To induce osteogenesis, the cells were seeded in 12-well culture plates and cultured in osteogenic induction medium: DMEM supplemented with 10% (v/v) FBS, 100 nM dexamethasone, and 50 mg ascorbic acid 2-phosphate/mL. Osteogenic differentiation was verified by staining with 0.5% (w/v) alizarin red S (ARS) (pH 4.1) after immobilization of isolated cells in 4% (v/v) paraformaldehyde for 10 min.

Data statistical analysis

All experiments were repeated at least five times, with similar results. All results are presented as the mean \pm standard deviation. Data were analyzed using analysis of variance (AN-

OVA) and Dunnett's t-test. Differences were considered statistically significant at $P < 0.05$. All statistical analyses were implemented with SPSS 20.0 software (SPSS Inc., Chicago IL, USA).

Results

Establishment and characteristics of the IM in rats

The establishment of Masquelet's IM in the femoral defect site is illustrated in **Figure 1A-C**. X-ray imaging showed good implantation of the PMMA spacer after surgery (**Figure 1D**). Hematoxylin and eosin staining of membrane tissue collected 6 weeks after surgery revealed an inner layer with intensive fibrous tissue and an outer layer with loose connective tissue and micro-vessels (**Figure 1E**). Immunohistochemical staining of BMP-2 and TGF- β revealed that the IM was a natural carrier of both BMP-2 and TGF- β (**Figure 1F** and **1G**).

Effect of the IM on the osteogenic differentiation of BMSCs

As shown in **Figure 2A**, qRT-PCR revealed that BMSCs treated with protein extract from IM and BMP-2 both exhibited higher mRNA expression level of Runx2 after 7, 14, and 21 days

Induced membrane and osteogenic differentiation

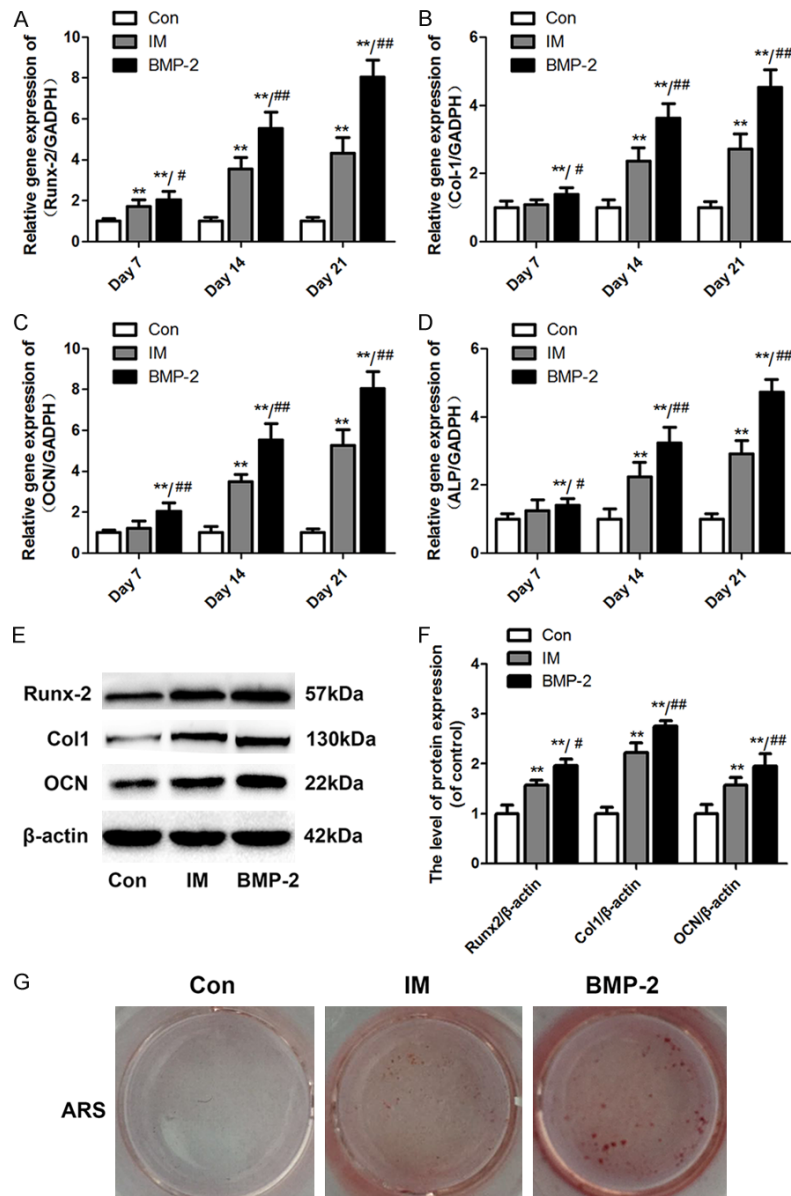


Figure 2. Induced membrane promotes the osteogenic differentiation of BMSCs. The cells osteogenic differentiation activity was assessed via qRT-PCR for Runx2, Col I, OCN, and ALP mRNA expression, western blotting for Runx2, Col I, and OCN protein expressions and Alizarin red staining (ARS) for calcium deposition after 14 days of culture. A-D: The mRNA expression levels of Runx2, Col I, OCN, and ALP in BMSCs treated with the IM or BMP-2 were calculated by normalizing the quantified mRNA amount to GADPH. E: Effect of the IM and BMP-2 on the protein expression of Runx2, Col I, and OCN. F: Optical density values of Runx2, Col I, and OCN expression were quantified and analyzed in each group. G: Formed calcium nodules in BMSCs treated with the IM or BMP-2 were colored red by ARS. Data in the figures represent the average \pm standard deviation (S.D.). Significant differences between groups are indicated as **P < 0.01, vs. control group, ##P < 0.01, vs. IM group. For each group, n = 5.

not reach significance in the IM group on day 7 (**Figure 2B-D**). Western blot analysis also revealed that both the IM and BMP-2 exert a significant effect on the protein expression of Runx2, Col 1, and OCN, particularly in the BMP-2 group (**Figure 2E and 2F**). Alizarin red staining was consistent with the PCR and western blot results (**Figure 2G**).

Effect of the IM on activation of the Smad1/5/8 and MAPK pathways in BMSCs

To investigate the molecular mechanism of IM-mediated osteogenic differentiation, the phosphorylation levels of Smad1/5/8 and related proteins involved in the MAPK pathway were examined. The IM promoted the phosphorylation of Smad1/5/8, ERK1/2, p38, and JNK (**Figure 3A-D**). Furthermore, specific inhibitors of Smad1/5/8 (LDN-193189) and ERK1/2 (UO-126) were applied to confirm these effects on IM-induced osteogenesis. The phosphorylation of Smad1/5/8 and ERK1/2 was significantly inhibited by LDN-193189 and UO126, respectively (**Figure 4A and 4B**). Moreover, the addition of both LDN-193189 and UO126 abolished the IM-induced increase in the expression of Runx2, Col 1, and OCN (**Figure 4C and 4D**).

Discussion

compared to the control group. Additionally, an increasing trend in the mRNA expression level of Col I, OCN and ALP was observed in the IM and BMP-2 groups, although the difference did

The reconstruction of large bone defects caused by trauma, infection, or other diseases with extensive bone loss is a challenging problem in clinical practice [3-5, 22]. Masquelet's

Induced membrane and osteogenic differentiation

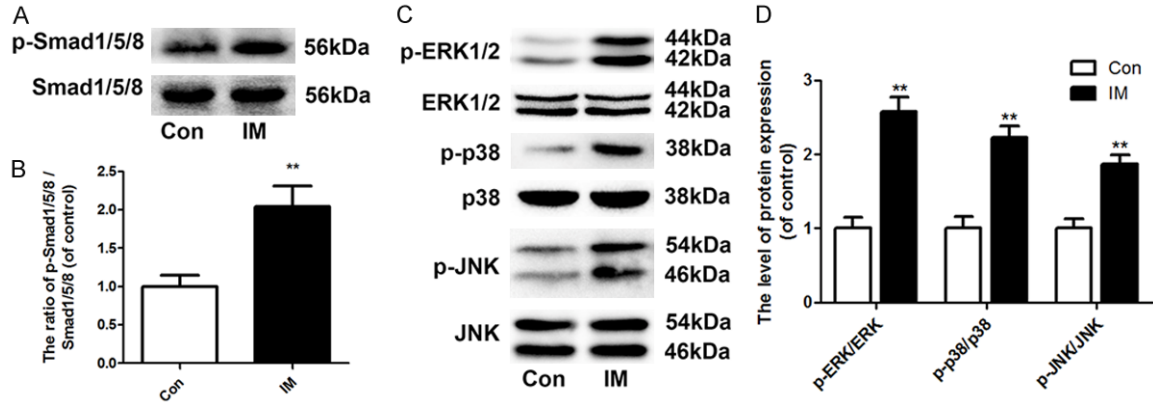


Figure 3. Induced membrane activates the Smad and MAPK pathways in BMSCs. The activation of the Smad and MAPK pathways were assessed via western blotting for the phosphorylation level of Smad1/5/8, ERK1/2, p38, and JNK protein after 14 days of culture. A: Effect of the IM on the phosphorylation of Smad1/5/8. B: Optical density values of the phosphorylation of Smad1/5/8 were quantified and analyzed in each group. C: Effect of the IM on the phosphorylation of ERK1/2, p38, and JNK. D: Optical density values of the phosphorylation of ERK1/2, p38, and JNK were quantified and analyzed in each group. Data in the figures represent the average \pm S.D. Significant differences between groups are indicated as $**P < 0.01$, vs. control group. For each group, $n = 5$.

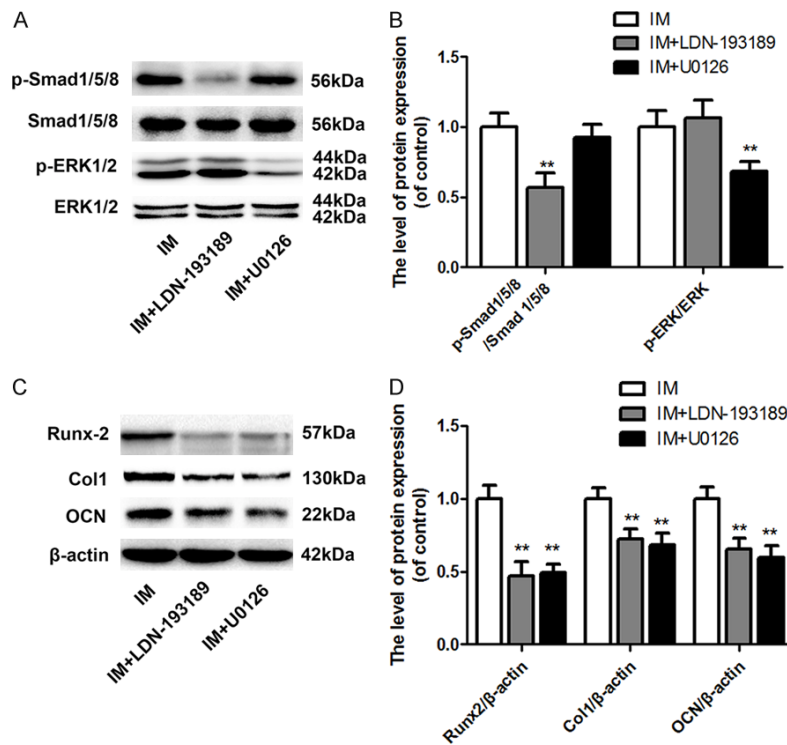


Figure 4. Inhibition of the Smad and MAPK pathways abolished IM-induced osteogenesis. The activation of the Smad and MAPK pathways and cells osteogenic differentiation activity were assessed via western blotting for the phosphorylation level of Smad1/5/8 and ERK1/2 protein and Runx2, Col I, and OCN protein expressions after 14 days of culture. A: Effect of the IM combined with LDN-193189 or U0126 on the phosphorylation of Smad1/5/8 and ERK1/2. B: Optical density values of the phosphorylation of Smad1/5/8 and ERK1/2 were quantified and analyzed in each group. C: Effect of the IM combined with LDN-193189 or U0126 on the protein expression of Runx2, Col I, and OCN. D: Optical density values of Runx2, Col I, and OCN expression were quantified and

analyzed in each group. Data in the figures represent the average \pm S.D. Significant differences between groups are indicated as $**P < 0.01$, vs. control group. For each group, $n = 5$.

IM acts as a biological chamber to promote bone graft vascularity and corticalization while inhibiting its resorption [9]. Thus, targeting this special tissue offers new possibilities for obtaining effective outcomes in the administration of large bone defects. Our former study and several other preclinical experiments in animal models have demonstrated that the IM significantly supports bone formation [23-25]. Moreover, Erwan de Monès et al. reported a significant increase in ALP expression in human BMSCs treated with protein extract from the IM [14]. However, few *in vitro* studies have focused on the molecular mechanism involved in its promo-

tion on osteogenesis. In the current study, we used BMP-2 as a positive control to evaluate the benefits of the IM in BMSCs osteogenic differentiation by examining the expression of osteogenic markers (i.e., Runx2, Col I, OCN, and ALP) via qRT-PCR and western blot analysis. Alizarin red staining, another golden standard used to evaluate BMSCs osteogenesis *in vitro*, was also performed to assess calcium-rich deposits.

Runx2 is one of the most essential transcription factors required for osteogenesis during BMSCs differentiation [26]. A deficiency in the Runx2 gene is reported as a cause of the human disease cleidocranial dysplasia, which is an autosomal dominant bone disorder [27]. Besides, the oncogenic properties of Runx2 have been demonstrated in a critical-size femoral defect model where Runx2 overexpression enhanced the osteoblastic differentiation and mineralization of BMSCs and thereby accelerated bone formation in final [28]. Following Runx2 activation, the up-regulation of both Col I (an early marker of osteogenesis) and OCN (a late marker of osteogenesis) was also observed [29]. In our study, although the beneficial effects of the IM on the expression of Runx2, Col I, and OCN were not as significant as BMP-2, the membrane was considerably effective compared with the untreated group. These results indicate that the induced membrane is a valid promoter to BMSCs osteogenic differentiation.

The histology, cellular makeup, and growth factor expression of the IM has been well studied. Growth factors such as BMP-2 and TGF- β , main components secreted from the IM, greatly contribute to bone formation [15]. Although several signaling pathways, including MAPK, Wnt/ β -catenin, phosphatidylinositide-3 kinase (PI3K)/Akt, and Smad, play a crucial role in BMSCs osteogenesis [19, 30-32], the Smad and MAPK pathways were reported significantly increasing Runx2 expression following induction with TGF- β and BMP-2 [20]. Thus, we examined whether these two pathways are involved in the IM-mediated osteogenic effect. The phosphorylation of Smad1/5/8 and MAPK cascades were increased after co-culturing MSCs with protein extract from the IM. Furthermore, the Smad inhibitor LDN-294002 and the ERK1/2 inhibitor U0126 were added after IM treatment, and the combination of inhibitors abolished the

osteogenic effect of the IM respectively which further suggested that the IM supports MSC osteogenic differentiation by enhancing Smad and MAPK activation.

In conclusion, the current study demonstrated that protein extract from the IM induced the phosphorylation of Smad and MAPK proteins, which subsequently activated the transcription of Runx2 to promote the osteogenic differentiation of BMSCs. Specific inhibition of the Smad and ERK1/2 MAPK pathways reduced IM-mediated osteogenesis. Therefore, our study revealed a deep association between Masquelet's IM and bone formation.

Acknowledgements

This study was supported by National Natural Science Foundation of China (NO. 81501869, NO. 81601983, NO. 41506091), Medical and health science and technology project of Zhejiang Province (2016YKA139), and Zhejiang provincial Public welfare project (2017C33035).

Disclosure of conflict of interest

None.

Address correspondence to: Dr. Haixiao Liu, Department of Orthopaedic Surgery, The Second Affiliated Hospital and Yuying Children's Hospital of Wenzhou Medical University, 109, Xueyuanxi Road, Wenzhou 325027, China. Tel: 86-577-88002808; Fax: 86-577-88816191; E-mail: spineliu@163.com

References

- [1] Masquelet AC, Fitoussi F, Begue T, Muller GP. [Reconstruction of the long bones by the induced membrane and spongy autograft]. *Ann Chir Plast Esthet* 2000; 45: 346-353.
- [2] Masquelet AC. Muscle reconstruction in reconstructive surgery: soft tissue repair and long bone reconstruction. *Langenbecks Arch Surg* 2003; 388: 344-346.
- [3] Aparad T, Bigorre N, Cronier P, Duteille F, Bizot P and Massin P. Two-stage reconstruction of post-traumatic segmental tibia bone loss with nailing. *Orthop Traumatol Surg Res* 2010; 96: 549-553.
- [4] Bus MP, Bramer JA, Schaap GR, Schreuder HW, Jutte PC, van der Geest IC, van de Sande MA and Dijkstra PD. Hemicortical resection and inlay allograft reconstruction for primary bone tumors: a retrospective evaluation in the Netherlands and review of the literature. *J Bone Joint Surg Am* 2015; 97: 738-750.

Induced membrane and osteogenic differentiation

- [5] Mauffrey C, Hake ME, Chadayammuri V and Masquelet AC. Reconstruction of long bone infections using the induced membrane technique: tips and tricks. *J Orthop Trauma* 2016; 30: e188-193.
- [6] Han W, Shen J, Wu H, Yu S, Fu J and Xie Z. Induced membrane technique: advances in the management of bone defects. *Int J Surg* 2017; 42: 110-116.
- [7] Auregan JC and Begue T. Induced membrane for treatment of critical sized bone defect: a review of experimental and clinical experiences. *Int Orthop* 2014; 38: 1971-1978.
- [8] Masquelet AC, Fitoussi F, Begue T and Muller GP. Reconstruction of the long bones by the induced membrane and spongy autograft. *Ann Chir Plast Esthet* 2000; 45: 346-353.
- [9] Masquelet AC and Begue T. The concept of induced membrane for reconstruction of long bone defects. *Orthop Clin North Am* 2010; 41: 27-37; table of contents.
- [10] Masquelet AC and Obert L. Induced membrane technique for bone defects in the hand and wrist. *Chir Main* 2010; 29 Suppl 1: S221-224.
- [11] Gan AW, Puhaindran ME and Pho RW. The reconstruction of large bone defects in the upper limb. *Injury* 2013; 44: 313-317.
- [12] Zwetyenga N, Fricain JC, De Mones E and Gindraux F. Induced membrane technique in oral & maxillofacial reconstruction. *Rev Stomatol Chir Maxillofac* 2012; 113: 231-238.
- [13] Henrich D, Seebach C, Nau C, Basan S, Relja B, Wilhelm K, Schaible A, Frank J, Barker J and Marzi I. Establishment and characterization of the Masquelet induced membrane technique in a rat femur critical-sized defect model. *J Tissue Eng Regen Med* 2016; 10: E382-E396.
- [14] de Mones E, Schlaubitz S, Oliveira H, d'Elbee JM, Bareille R, Bourget C, Couraud L and Fricain JC. Comparative study of membranes induced by PMMA or silicone in rats, and influence of external radiotherapy. *Acta Biomater* 2015; 19: 119-127.
- [15] Pelissier P, Masquelet AC, Bareille R, Pelissier SM and Amedee J. Induced membranes secrete growth factors including vascular and osteoinductive factors and could stimulate bone regeneration. *J Orthop Res* 2004; 22: 73-79.
- [16] Klimczak A and Kozłowska U. Mesenchymal stromal cells and tissue-specific progenitor cells: their role in tissue homeostasis. *Stem Cells Int* 2016; 2016: 4285215.
- [17] Bruder SP, Fink DJ, Caplan AI. Mesenchymal stem cells in bone development, bone repair, and skeletal regeneration therapy. *J Cell Biochem* 1994; 56: 283-294.
- [18] Artigas N, Urena C, Rodriguez-Carballo E, Rosa JL and Ventura F. Mitogen-activated protein kinase (MAPK)-regulated interactions between Osterix and Runx2 are critical for the transcriptional osteogenic program. *J Biol Chem* 2014; 289: 27105-27117.
- [19] Rath B, Nam J, Deschner J, Schaumburger J, Tingart M, Grassel S, Grifka J and Agarwal S. Biomechanical forces exert anabolic effects on osteoblasts by activation of SMAD 1/5/8 through type 1 BMP receptor. *Biorheology* 2011; 48: 37-48.
- [20] Wu M, Chen G and Li YP. TGF-beta and BMP signaling in osteoblast, skeletal development, and bone formation, homeostasis and disease. *Bone Res* 2016; 4: 16009.
- [21] Tropel P, Noel D, Platet N, Legrand P, Benabid AL and Berger F. Isolation and characterisation of mesenchymal stem cells from adult mouse bone marrow. *Exp Cell Res* 2004; 295: 395-406.
- [22] Lasanianos NG, Kanakaris NK and Giannoudis PV. Current management of long bone large segmental defects. *Orthopaedics and Trauma* 2010; 24: 149-163.
- [23] Bosemark P, Perdikouri C, Pelkonen M, Isaksson H and Tägil M. The masquelet induced membrane technique with BMP and a synthetic scaffold can heal a rat femoral critical size defect. *J Orthop Res* 2015; 33: 488-495.
- [24] Liu H, Hu G, Shang P, Shen Y, Nie P, Peng L and Xu H. Histological characteristics of induced membranes in subcutaneous, intramuscular sites and bone defect. *Orthop Traumatol Surg Res* 2013; 99: 959-964.
- [25] Viateau V, Guillemin G, Bousson V, Oudina K, Hannouche D, Sedel L, Logeart-Avramoglou D and Petite H. Long-bone critical-size defects treated with tissue-engineered grafts: a study on sheep. *J Orthop Res* 2007; 25: 741-749.
- [26] Zhao Z, Zhao M, Xiao G and Franceschi RT. Gene transfer of the Runx2 transcription factor enhances osteogenic activity of bone marrow stromal cells in vitro and in vivo. *Mol Ther* 2005; 12: 247-253.
- [27] Ott CE, Leschik G, Trotier F, Brueton L, Brunner HG, Brussel W, Guillen-Navarro E, Haase C, Kohlhase J, Kotzot D, Lane A, Lee-Kirsch MA, Morlot S, Simon ME, Steichen-Gersdorf E, Tegay DH, Peters H, Mundlos S and Klopocki E. Deletions of the RUNX2 gene are present in about 10% of individuals with cleidocranial dysplasia. *Hum Mutat* 2010; 31: E1587-1593.
- [28] Wojtowicz AM, Templeman KL, Hutmacher DW, Guldberg RE and Garcia AJ. Runx2 overexpression in bone marrow stromal cells accelerates bone formation in critical-sized femoral defects. *Tissue Eng Part A* 2010; 16: 2795-2808.
- [29] Franceschi RT and Xiao G. Regulation of the osteoblast-specific transcription factor, Runx2: responsiveness to multiple signal transduction pathways. *J Cell Biochem* 2003; 88: 446-454.
- [30] Simann M, Le Blanc S, Schneider V, Zehe V, Ludemann M, Schutze N, Jakob F and Schilling

Induced membrane and osteogenic differentiation

- T. Canonical FGFs prevent osteogenic lineage commitment and differentiation of human bone marrow stromal cells via ERK1/2 signaling. *J Cell Biochem* 2017; 118: 263-275.
- [31] Baker N, Sohn J and Tuan RS. Promotion of human mesenchymal stem cell osteogenesis by PI3-kinase/Akt signaling, and the influence of caveolin-1/cholesterol homeostasis. *Stem Cell Res Ther* 2015; 6: 238.
- [32] Tornero-Esteban P, Peralta-Sastre A, Herranz E, Rodriguez-Rodriguez L, Mucientes A, Abasolo L, Marco F, Fernandez-Gutierrez B and Lamas JR. Altered expression of Wnt signaling pathway components in osteogenesis of mesenchymal stem cells in osteoarthritis patients. *PLoS One* 2015; 10: e0137170.